PROCEEDINGS OF SPIE

SPIEDigitalLibrary.org/conference-proceedings-of-spie

Multifocal structured illumination fluorescence microscopy with large field-of-view and high spatio-temporal resolution

Zhenyue Chen, Ben Mc Larney, Johannes Rebling, Xosé Luis Deán-Ben, Sven Gottschalk, et al.

Zhenyue Chen, Ben Mc Larney, Johannes Rebling, Xosé Luis Deán-Ben, Sven Gottschalk, Daniel Razansky, "Multifocal structured illumination fluorescence microscopy with large field-of-view and high spatio-temporal resolution," Proc. SPIE 10816, Advanced Optical Imaging Technologies, 1081606 (5 November 2018); doi: 10.1117/12.2500907



Event: SPIE/COS Photonics Asia, 2018, Beijing, China

Multifocal structured illumination fluorescence microscopy with large field-of-view and high spatio-temporal resolution

Zhenyue Chen^a, Ben Mc Larney, a,b Johannes Rebling, a,b Xosé Luís Deán-Ben^a, Sven Gottschalk^a, and Daniel Razansky^{a,b,*}

^a Institute for Biological and Medical Imaging (IBMI), Helmholtz Center Munich, Ingolstaedter Landstr. 1, 85764 Neuherberg, Germany.

ABSTRACT

Fluorescence imaging is widely employed in biological discovery due to its excellent molecular sensitivity and contrast. However, due to light scattering wide-field fluorescence images are blurred resulting in very low spatial resolution and low image contrast. The existing scanning optical microscopy techniques are commonly restricted to sub-millimeter field-of-view or otherwise slow imaging speeds, limiting their applicability for imaging of fast biological dynamics occurring on larger spatial scales. Herein, we developed a rapid scanning wide-field multifocal structured illumination microscopy method based on a beam-splitting grating and an acousto-optic deflector synchronized with a high speed camera. The multi-beam pattern is focused by a condensing lens and a macroscopic objective to generate multifocal structured illumination profile on the imaged sample that is rapidly scanned at kHz rates. Experimental results show that the proposed method can achieve real-time fluorescence microscopy over a centimeter-scale field of view. Owing to the low numerical aperture of the diffracted beams, the illumination has a large depth of focus and hence is generally not affected by the sample's curvature, which allowed here imaging of perfusion in the entire mouse cerebral cortex noninvasively. The new approach can be readily incorporated into traditional wide-field microscopes to attain optimal tradeoff between spatial resolution and field of view. It further establishes a bridge between conventional wide-field macroscopy and laser scanning confocal microscopy, thus anticipated to find broad applicability in a variety of applications looking at large-scale fluorescent-based biodynamics.

Keywords: fluorescence imaging, multifocal structured illumination, large field of view, high speed

1. INTRODUCTION

Owing to its high molecular specificity, excellent contrast and spatial resolution, fluorescence microscopy has become a workhorse of the modern biological discovery [1-9]. With the advent of high speed cameras, wide-field fluorescence microscopes are now capable of achieving kilohertz (kHz) imaging speeds when tracking fast biological dynamics. However, the effective resolving capacity of traditional wide-field microscopes is severely impaired when imaging through scattering objects [10]. Also, high photo-bleaching rates associated with continuous light exposure of the entire imaged sample hamper observations of longitudinal dynamics [11].

The effects of scattering and photobleaching in fluorescent microscopy can be minimized by employing scanning-based approaches. To this end, abundance of scanning microscopy techniques have been developed and are widely used in biomedical research [12-17]. In single point scanning methods, such as laser scanning confocal microscopy (LSCM) [18, 19] or two-photon microscopy (2PM) [20, 21], the fluorescent signal is selectively generated or detected from a diffraction-limited focal spot. Stimulated emission depletion (STED) microscopy has further enabled breaking through the optical diffraction barrier by attaining super-resolution imaging [13, 22]. Single point scanning methods are however not suitable for imaging fast processes and efforts are underway to boost imaging speeds by employing fast-scanning components, such as mechanical stages, micro-electro-mechanical systems (MEMS), galvanometer mirrors and acoustooptic deflectors [23-29].

^b Faculty of Medicine, Technical University of Munich, Ismaninger Str. 22, 81675 Munich, Germany.

^{*}Corresponding author: dr@tum.de

The imaged field of view (FOV) that can be efficiently covered per unit time is further determined by the size of the focal light spot. Thus, volumetric imaging rates can be ramped up by giving up on the spatial resolution [30]. For example, the focal spot in 2PM can be smeared using sculpted light [31]. Recent efforts in optical microscopy have additionally been devoted to other methodologies that attain high-frame-rate volumetric imaging, e.g. light sheet [32, 33] or light field [34, 35] microscopy. Hybrid opto-acoustic tomography and microscopy systems have recently demonstrated powerful large-scale volumetric imaging performance [36, 37], outperforming the speed [38] and sensitivity of fluorescence readings at deeper locations in living scattering tissues [39].

Parallel acquisition methods represent an alternative approach for accelerating imaging by simultaneously illuminating larger areas or generating multiple foci. For instance, spinning disk confocal microscopy (SDCM) utilizes multiple pinholes or slits to project a series of 1000 or more parallel excitation foci onto the sample in a multiplexed pattern [40, 41]. Parallelized multi-beam STED has enabled video-rate nanoscopy recordings by speeding up imaging by a factor of 2000 [42]. Simultaneous scanning of separate regions has been suggested for visualizing large areas with 2PM [43]. Structured illumination microscopy (SIM) arguably offers the highest degree of parallelization as only a relatively small number of wide-field images are required for rendering a super-resolution image. State-of-the-art SIM can achieve imaging rates of 79 frames per second for a region of interest (ROI) of 16.5 x 16.5 μ m² [44]. Recent progress on multifocal SIM enabled three dimensional (3D) interrogation of live organisms at frame rates of ~1 Hz, covering a FOV in the 50 -100 μ m range [45-47]. In general, parallel acquisition methods are only applicable for imaging very small areas with high resolution, so that wide-field approaches remain the method of choice for large-scale imaging.

Here we propose a wide-field multifocal structured illumination scanning microscopy method based on an acousto-optic deflector (AOD) and a beam-splitting grating. The laser beam is raster scanned by the AOD running at kHz scanning rate with the beam split into hundreds of mini-beams, which are subsequently focused by a condensing lens and a macroscopic objective to generate multifocal structured illumination. The excited fluorescence signal is synchronously collected by a high speed camera with the signals then combined into a high resolution image.

2. METHODS

2.1 System setup

Figure 1 depicts the schematic diagram of the proposed multifocal structured illumination microscopy system. A high pulse repetition frequency (PRF) Q-switched, diode end-pumped Nd:YAG laser (model: IS8II-E, EdgeWave, Germany) operating at 532 nm wavelength was used for excitation. The PRF of the laser is adjustable within the 200 Hz - 10 kHz range. The laser beam was first scanned by the AOD (AA Opto-Electronic, France) and then guided into a customized beam-splitting grating (Holoeye GmbH, Germany) to generate multiple mini-beams. The custom-made gratings were manufactured with different diffraction orders, such as $-7 \sim +7$ orders and $-10 \sim +10$ orders, and have a diffraction efficiency of \sim 74% and intensity uniformity within $\pm 10\%$ for all the diffraction orders. The angle between adjacent diffraction orders is 0.57°, smaller than the maximum scanning angle of 2.292° of the AOD. In Fig. 1(a), the system is integrated into a wide-field microscopy system, where the mini-beams are relayed by Lens 1 and Lens to the input pupil of the microscope objective and then get focused onto the sample to generate multiple foci. In Fig. 1(b), the system is built based on a wide-field macroscopy system, where the mini-beams are relayed by Lens 1 and focused by a microlens with tunable focal length and the excited fluorescence signal is collected by a micro-lens as labeled as Lens 3 and then focused onto the sensor plane of a high speed camera (PCO AG, Germany). The PCO camera has frame rate up to 4467 fps at full pixel resolution of 1008 x 1008 pixels. During data acquisition, a NI-PCIe 6535b DIO (National Instrument, USA) was employed to synchronize the data transfer of the AOD and trigger signals for the laser pulse and camera acquisition. Since the AOD has 15-bit scanning accuracy within the full scan angle, raster scanning or random scanning the multifocal structured illumination pattern both in horizontal and vertical planes results in a high resolution image. Note that, the system design in Fig. 1(a) employs the on-axis illumination which makes the illumination plane always same to the image plane of the system. However, the imaged FOV is limited by the numerical aperture (NA) of the microscope objective and its work distance. On the contrary, for the system shown in Fig. 1(b) the illumination plane has to be adjusted independently so that it will reside on the same plane to the imaging plane. The advantage of this design is the imaged FOV can be adjusted very conveniently bas adjusting the work distance of Lens 2. The experimental results in the following sections are based on the design in Fig. 1(b).

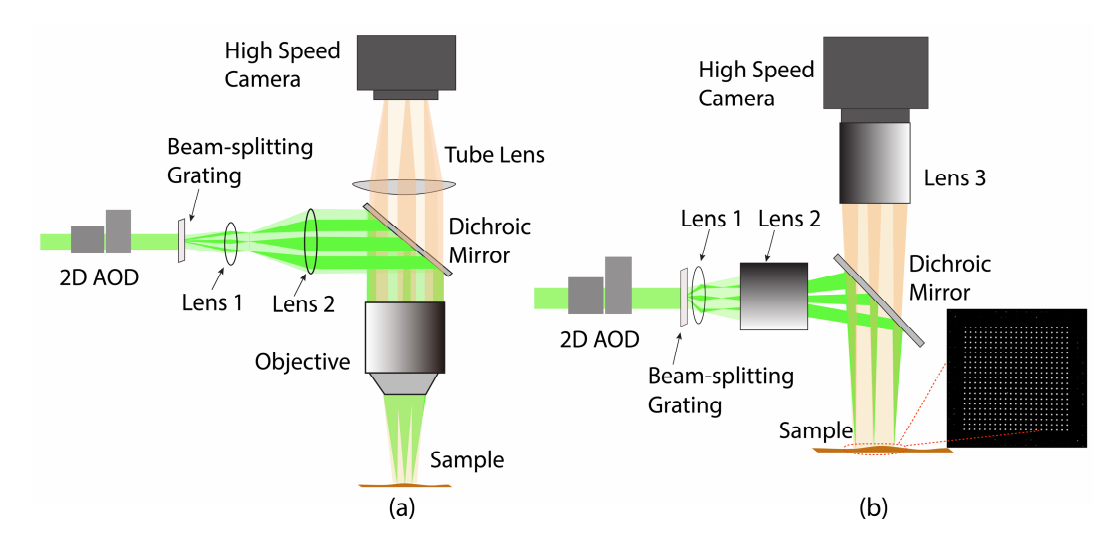


Figure 1 Schematic diagram of the wide-field multifocal structured illumination system consisting of an acousto-optic deflector (AOD), beam-splitting grating, focusing assembly, and a high-speed fluorescence camera. (a) System setup based on a wide-field microscope. (b) System setup based on a macroscopic imaging system. The inset in the bottom right corner in (b) shows the illumination grid when a 21x21 beam-splitting grating is employed. In this case, an inter-beam angle of 0.57° is achieved while raster scanning the multifocal structured illumination pattern both in horizontal and vertical planes renders a high-resolution image over a large FOV of 20 x 20 mm².

2.2 In vivo experiment

The proposed method was validated in vivo by imaging the brain of a 3-month old athymic nude-Fox1nu mouse (Harlan Laboratories LTD, Switzerland) following a tail-vein injection of 10 μl of 1 mg/ml (~138 μM) Alexa FluorTM 532 carboxylic acid (Thermo Fisher Scientific, USA) solution in water. A 21x21 beam-splitting grating and a 35 mm planoconvex lens and a Nikkor 35mm f/2D lens (Lens 1) were employed to generate the multifocal structured illumination pattern. A 2-inch dichroic mirror (DMLP567L, Thorlabs, USA) separated the emission light from the excitation. A Nikon 105mm f/2.8D AF Micro Nikkor lens (Lens 2) collected the emitted signal. The mouse was anesthetized with isoflurane (2.5% v/v for induction and 1.5-2.0% v/v during experiments) in 100% O2 at a flow rate of ~0.8 l/min. The skull of the mouse was kept intact while the scalp was removed to reduce light scattering. In this case, to minimize bleeding, hemostatic sponges (Gelfoam®, Pfizer Pharmaceutical) were used together with a topical application of adrenaline. After the experiment the animal was euthanized while still being under anesthesia. Animal handling and experimentation were conducted in full accordance with the directives on animal experimentation of the Helmholtz Center Munich and with approval from the Government District of Upper Bavaria. The same imaging set-up was used for both phantom and in vivo experiments. However, in the latter case only 15 x 15 scanning steps were employed in order to increase the imaging speed. The laser output after the diffraction grating was increased to ~500 μJ/pulse to compensate for a relatively weak fluorescent signal and strong scattering by different tissue layers. After concluding the data acquisition, the mouse received second dye injection while fluorescence images were recorded with conventional wide-field fluorescence method for comparison.

3. RESULTS AND DISCUSSION

The performance of the proposed multifocal structured illumination microscopy method was compared with that of conventional wide-field method in simulation. The simulation results are displayed in Fig. 2. Fig. 2a displays the ground truth image with high image contrast and spatial resolution. By applying a low pass filter to the imaging system, a point spread function (PSF) was obtained to simulate the light diffusion effect and the zoom-in of the PSF is shown in Fig. 2b. Fig. 2c shows one scanning frame after applying the PSF to the product of the 21x21 structured illumination and the ground truth sample. Fig. 2d shows the corresponding deconvoluted image of Fig. 2c. Fig. 2e shows the convoluted image of the PSF (Fig. 2b) and the ground truth image (Fig. 2a) to simulate the wide-field image. Fig. 2f shows the deconvoluted image after applying image deconvolution to Fig. 2e. Fig. 2g shows the reconstructed image by stitching 20x20 scanning frames. For each frame, only the signal from the central pixel of each illumination spot is extracted. Fig. 2h shows the reconstructed image by further applying image deconvolution to each scanning frame before signal

stitching. Fig. 2i shows the signal profile comparison of Fig. 2a and Figs. 2e – 2i along the red line as indicated in Fig. 2h. From the signal profiles in Fig. 2i, we can see that the proposed method can improve image contrast and spatial resolution by reducing light scattering. It is also seen that by applying image deconvolution to each scanning frame before signal extraction, the spatial resolution of the reconstructed image (Fig. 2h) can be further improved. However, in real experiments, the PSF of the system is not accurately known and it may be different in different imaged regions. So for image reconstruction, we just simply stitched the signals from the central pixel of each illumination spot without applying image deconvolution.

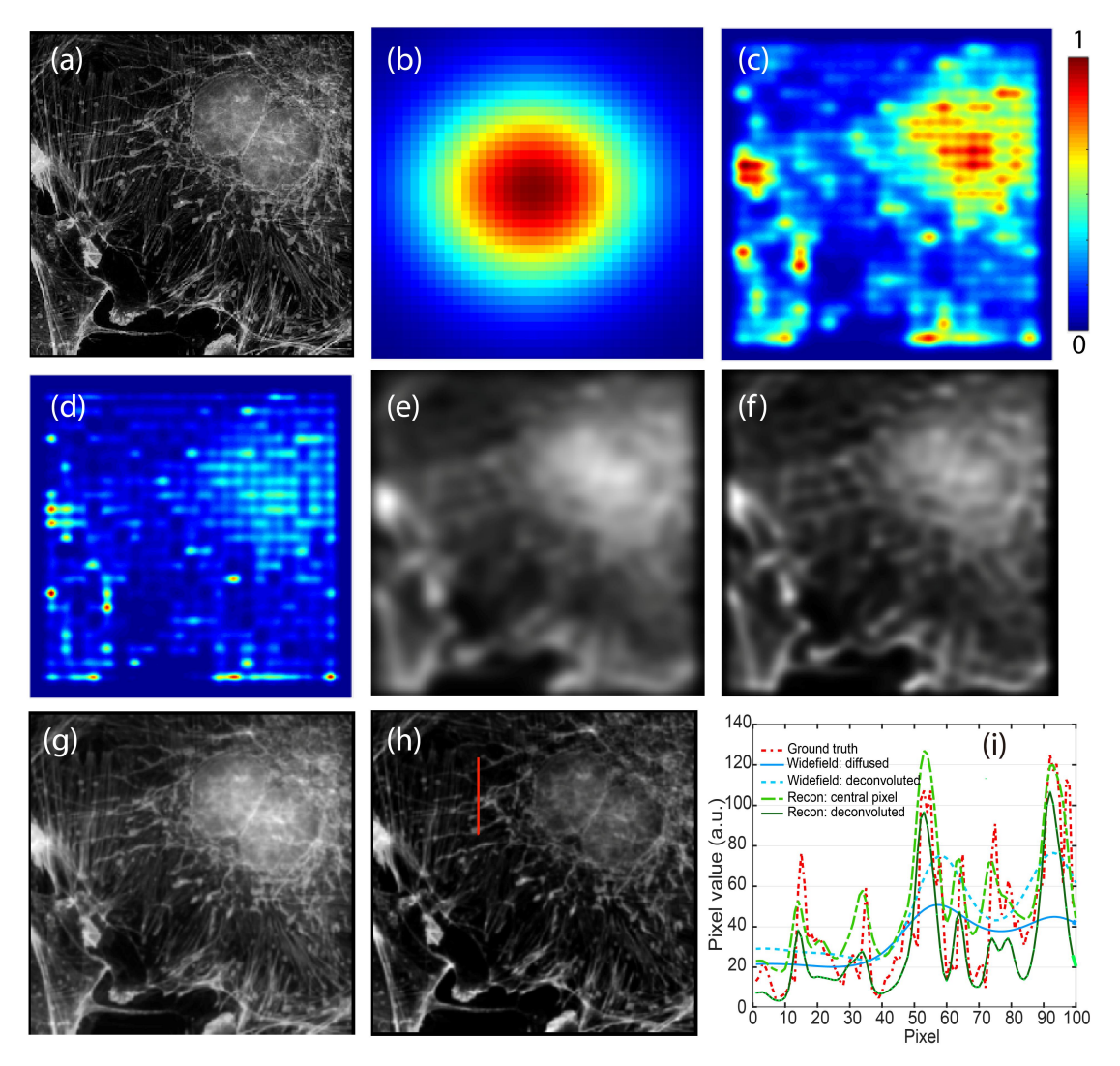


Figure 2 Performance comparison between the proposed method and conventional wide-field methods in simulation. (a) Ground truth image. (b) Diffused image by applying low pass filter to the ground truth image in (a). (c) Deconvoluted wide-field image after applying image deconvolution to the diffused image shown in (b). (d) Reconstructed image based on the multifocal structured illumination method by simply stitching the signal of each illumination spot. (e) Reconstructed image by further applying deconvolution to the signal obtained from central pixel of each illumination spot. (f) Signal profile comparison of (a) – (e) along the red line as indicated in (e).

System characterization was performed before in vivo animal experiment. The grid pattern of the diffracted beam was measured with the beam profiler and it exhibited good uniformity with the individual spots having $\sim 20 \mu m$ diameter within ~ 1 mm DOF. To characterize the spatial resolution, $10 \mu m$ size fluorescence beads were measured. Our measurement showed that due to the magnification power of the 105 mm Nikon lens (i.e., Lens 3 in Fig. 1b), the effective spatial resolution achieved was $\sim 24.6 \mu m$ which was also dependent on the pixel size of the camera. Time-lapse

imaging results from the tail-vein injection of Alexa Fluor 532 fluorescent dye are shown in Fig. 3. Note that the in vivo experiment was performed transcranially while the scalp was removed to reduce light scattering. As expected, the conventional wide-field images (Fig. 3a) are blurred due to the strong light scattering in the mouse brain, rendering its cerebral vascular anatomy indistinguishable. On the contrary, the reconstructed images acquired by combining 15 x 15 = 225 scanning steps (Fig. 3b) exhibit excellent contrast and spatial resolution through the intact skull while also accurately resolving the perfusion process in the deeply embedded cerebral microvasculature. The same average laser output power was used in both cases. We then reconstructed the entire vascular tree by combining maximum pixel intensities across the temporal reconstructed image sequence (Fig. 3c), encoding it as intensity and saturation [48]. Time to peak analysis (Fig. 3d) further reveals the contrasting perfusion behavior. For instance, the sinusoidal vascular networks, presumably belonging to the skull, exhibit much longer perfusion constants. Note that the significant spatial blurring of the conventional wide-field fluorescence also introduces smearing into the perfusion signal profiles (Fig. 3e) while signal profiles from reconstructed multifocal structured illumination based images (Fig. 3f) can better present the perfusion dynamics.

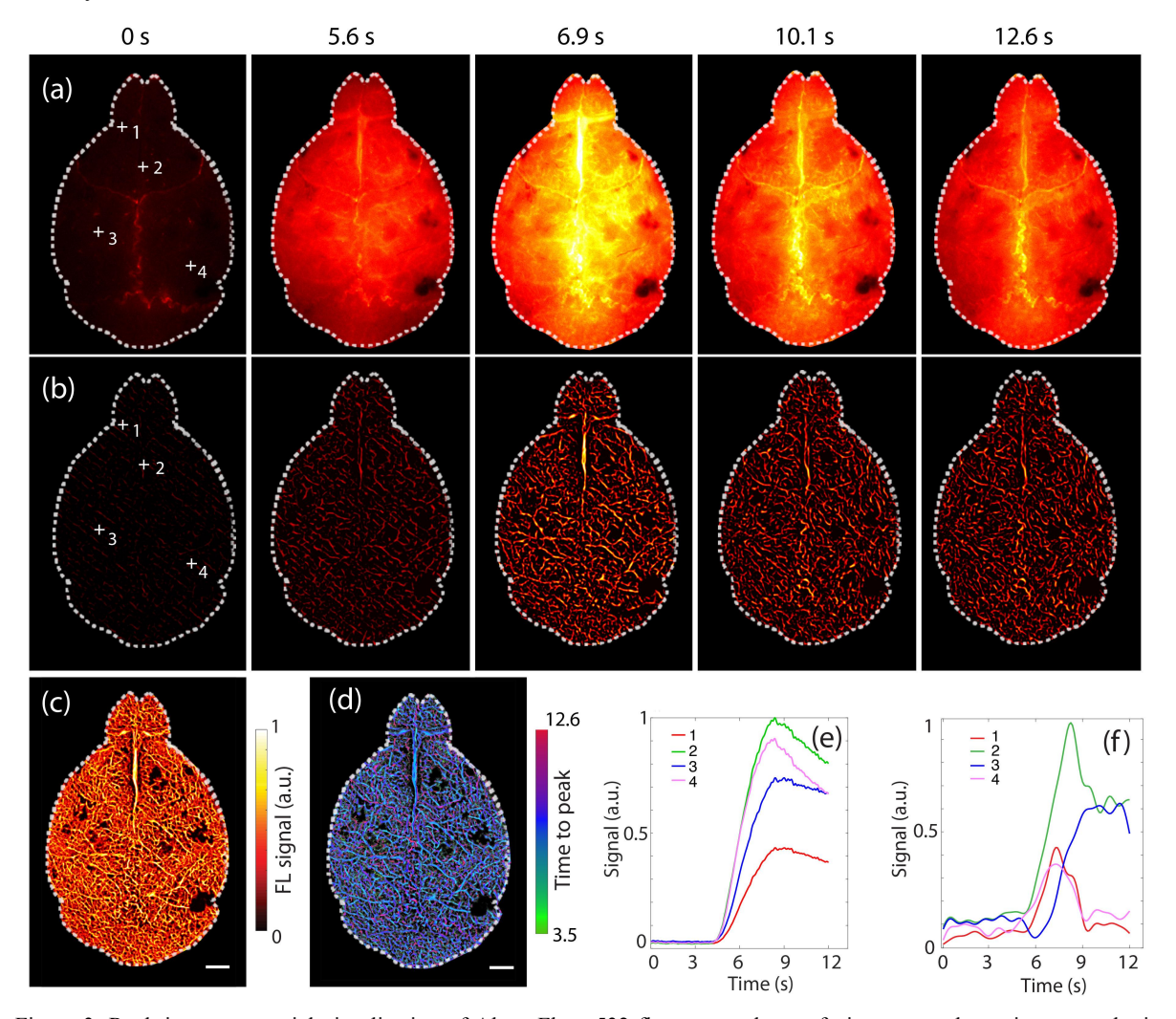


Figure 3. Real-time transcranial visualization of Alexa Fluor 532 fluorescent dye perfusion across the entire mouse brain cortex. (a) Time-lapse sequence of conventional wide-field fluorescence images. (b) The corresponding reconstructed image sequence acquired with a 15 x 15 scanning pattern, i.e. 10 frames per second full image rate at 2.25 kHz laser pulse repetition rate. (c) Temporal maximum intensity projection of the reconstructed image sequence, encoded as intensity and saturation. (d) The corresponding time to peak map. (e) Perfusion profiles in the corresponding areas of the wide-field fluorescence images, as indicated in panel (a). (f) Temporal signal profiles in individual pixels whose locations are indicated in panel (b). Scale bar 1 mm.

High temporal resolution is crucial when it comes to imaging rapid biological dynamics in e.g. freely behaving organisms, heart motion, fast perfusion, neural activity, to name a few examples. Imaging rates of conventional scanning optical microscopy methods are determined by the scanning speed of the laser beam. For instance, in MEMS- or piezobased scanning systems, the speed limitations chiefly arise from inertia associated with the mass of rotating mirrors and other moving parts. Modern AODs can achieve megahertz scanning speeds, thus allowing random access with high accuracy. Yet, their major drawback is the small deflection angles (typically < 0.05 rad) and limited resolvable number of spots (typically < 500) [49]. Here we capitalized instead on the large diffraction angle and the multi-beams strategy introduced by the beam-splitting grating. In this way, by employing 21x21 beam-splitting grating, the maximum deflection angle has been effectively expanded to 5.7° while the number of resolvable spots was increased by 21 fold.

The achievable image acquisition rate of the proposed method is mainly determined by the camera speed and the laser PRF. Thus, the effective frame rate can be further improved by: (1) Reducing the FOV so that less scanning steps are required to form one combined reconstructed image. Since commercial Nikon lenses are employed in the system, the illumination and imaging work distance can be readily adjusted to attain FOVs between 7 mm up to several centimeters across; (2) Employing a higher order beam-splitting grating (e.g. 101 x 101) would generate 10,201 individual beams, thus boosting the data acquisition rates by a factor of 23 as compared to the 21x21 grating only having 441 individual beams. Note that the output power of the laser has to be increased accordingly in this case; (3) Multiple scans of the illumination pattern can potentially be integrated to form one camera frame, as long as the adjacent spots are well separated in the integrated camera frame. In our current implementation, the laser has a PRF of up to 10 kHz and its pulse width is 10 ns whereas the high speed camera has a 4.4 kHz frame rate. By increasing the laser PRF, one may potentially render combined images at frame rates effectively limited by the camera speed. Furthermore, since thousands of foci are employed for simultaneous excitation in each scan, the pixel dwell time is accordingly increased thousands fold as compared to LSCM, resulting in tremendous improvement of the image SNR per given average power levels. Besides, due to the higher quantum efficiency of the high speed camera as compared with the photomultiplier tubes typically employed for the LSCM (QE < 40%), higher photon detection efficiency can be achieved, which will further reduce photobleaching and phototoxicity.

When comparing to SDCM, the proposed technique similarly employs multiple foci for the excitation. However, our proposed method is a more versatile, less complex to implement and easier to be adopted by wide-field microscopes. The pinhole diameters in SDCM are fixed, resulting in significant crosstalk between the neighboring pinholes. Therefore, one has to space the pinholes considerably to avoid crosstalk between the individual beams, which inevitably decreases the excitation light throughput [41]. Besides, the maximum imaging speed of SDCM is restricted to 1/12 of the spinning disk rotation frequency, leading to significantly slower scanning speed in comparison with AODs [41]. Although sinusoidal SIM techniques require fewer illumination patterns, they are unable to physically reject out-of-focus light, therefore optical sectioning is solely achieved with computational processing. In our proposed method, the out-of-focus background is inherently rejected (reduced) by the hardware. Additionally, due to the small NA of the individual pencil-like beams, the depth of focus of the illumination light is greatly increased, making the system especially powerful for imaging large samples with curved surfaces, such as the intact mouse brain.

4. CONCLUSIONS

In conclusion, we propose a rapid scanning fluorescence microscopy method based on multifocal structured illumination and acousto-optic beam steering. The powerful combination between large FOV (20 x 20 mm²), enhanced DOF (>1 mm), and real-time imaging performance has been achieved for the first time, to our best knowledge. The non-invasive in vivo mouse brain imaging results further demonstrate the superior performance of the proposed multifocal structured illumination microscopy method for imaging highly scattering, large scale object with a curved surface. The proposed method establishes a bridge between conventional wide-field macroscopy and laser scanning confocal microscopy, thus anticipated to find broad applicability in functional neuroimaging, in vivo tracking of cells and other applications looking at large-scale fluorescent-based biodynamics.

ACKNOWLEDGEMENT

The authors would like to thank M. Reiss and U. Klemm for the assistance in animal experimentation. This project has received funding from the European Union's Horizon 2020 research and innovation programme under the Marie

Skłodowska-Curie Grant Agreement No. 746430 - MSIOAM and the European Research Council Consolidator Grant ERC-2015-CoG-682379.

REFERENCES

- [1] G. C. H. Mo, "Genetically encoded biosensors for visualizing live-cell biochemical activity at super-resolution," NAT METHODS 14, 427-434 (2017).
- [2] C. Smith, M. Huisman, M. Siemons, D. Grunwald, and S. Stallinga, "Simultaneous measurement of emission color and 3D position of single molecules," OPT EXPRESS 24, 4996-5013 (2016).
- [3] B. J. Beliveau, "Single-molecule super-resolution imaging of chromosomes and in situ haplotype visualization using Oligopaint FISH probes," NAT COMMUN 6, 7147 (2015).
- [4] J. Ries, C. Kaplan, E. Platonova, H. Eghlidi, and H. Ewers, "A simple, versatile method for GFP-based super-resolution microscopy via nanobodies," NAT METHODS 9, 582-584 (2012).
- [5] P. Sengupta, "Probing protein heterogeneity in the plasma membrane using PALM and pair correlation analysis," NAT METHODS 8, 969-975 (2011).
- [6] C. A. Combs, and H. Shroff, "Fluorescence Microscopy: A Concise Guide to Current Imaging Methods," Curr Protoc Neurosci 79, 1-2 (2017).
- [7] J. W. Lichtman, and J. A. Conchello, "Fluorescence microscopy," NAT METHODS 2, 910-919 (2005).
- [8] C. A. Combs, and H. Shroff, "Fluorescence Microscopy: A Concise Guide to Current Imaging Methods," Curr Protoc Neurosci 79, 1-2 (2017).
- [9] J. W. Lichtman, and J. A. Conchello, "Fluorescence microscopy," NAT METHODS 2, 910-919 (2005).
- [10] V. Ntziachristos, "Going deeper than microscopy: the optical imaging frontier in biology," NAT METHODS 7, 603-614 (2010).
- [11] C. Boudreau, T. E. Wee, Y. S. Duh, M. P. Couto, K. H. Ardakani, and C. M. Brown, "Excitation Light Dose Engineering to Reduce Photo-bleaching and Photo-toxicity," SCI REP-UK 6, 30892 (2016).
- [12]B. Huang, S. A. Jones, B. Brandenburg, and X. Zhuang, "Whole-cell 3D STORM reveals interactions between cellular structures with nanometer-scale resolution," NAT METHODS 5, 1047-1052 (2008).
- [13] K. I. Willig, S. O. Rizzoli, V. Westphal, R. Jahn, and S. W. Hell, "STED microscopy reveals that synaptotagmin remains clustered after synaptic vesicle exocytosis," NATURE 440, 935-939 (2006).
- [14] E. Betzig, "Imaging intracellular fluorescent proteins at nanometer resolution," SCIENCE 313, 1642-1645 (2006).
- [15] M. J. Rust, M. Bates, and X. Zhuang, "Sub-diffraction-limit imaging by stochastic optical reconstruction microscopy (STORM)," NAT METHODS 3, 793-796 (2006).
- [16] M. Hofmann, C. Eggeling, S. Jakobs, and S. W. Hell, "Breaking the diffraction barrier in fluorescence microscopy at low light intensities by using reversibly photoswitchable proteins," Proc. Natl Acad. Sci. USA 102, 17565-17569 (2005).
- [17] M. G. L. Gustafsson, "Surpassing the lateral resolution limit by a factor of two using structured illumination microscopy," J. Microsc. 198, 82-87 (2000).
- [18] M. Minsky, "Memoir on inventing the confocal scanning microscope," SCANNING 10, 128-138 (1988).
- [19] S. Hell, and E. H. K. Stelzer, "Properties of a 4Pi confocal fluorescence microscope," J OPT SOC AM A 9, 2159-2166 (1992).
- [20] I. D. Abella, "Optical Double-Photon Absorption in Cesium Vapor," PHYS REV LETT 9, 453-455 (1962).
- [21] W. Kaiser, and C. G. B. Garrett, "Two-Photon Excitation in CaF2:Eu2+," PHYS REV LETT 7, 229-231 (1961).
- [22] T. A. Klar, S. Jakobs, M. Dyba, A. Egner, and S. W. Hell, "Fluorescence microscopy with diffraction resolution barrier broken by stimulated emission," Proc. Natl Acad. Sci. USA 97, 8206-8210 (2000).
- [23] J. Wu, A. H. L. Tang, A. T. Y. Mok, W. Yan, G. C. F. Chan, K. K. Y. Wong, and K. K. Tsia, "Multi-MHz laser-scanning single-cell fluorescence microscopy by spatiotemporally encoded virtual source array," BIOMED OPT EXPRESS 8, 4160-4171 (2017).
- [24] Q. Geng, C. Gu, J. Cheng, and S. Chen, "Digital micromirror device-based two-photon microscopy for three-dimensional and random-access imaging," OPTICA 4, 674-677 (2017).
- [25] J. Schneider, "Ultrafast, temporally stochastic STED nanoscopy of millisecond dynamics," NAT METHODS 12, 827-830 (2015).

- [26] R. Salomé, Y. Kremer, S. Dieudonné, J. F. Léger, O. Krichevsky, C. Wyart, D. Chatenay, and L. Bourdieu, "Ultrafast random-access scanning in two-photon microscopy using acousto-optic deflectors," J NEUROSCI METH 154, 161-174 (2006).
- [27] W. Göbel, B. M. Kampa, and F. Helmchen, "Imaging cellular network dynamics in three dimensions using fast 3D laser scanning," NAT METHODS 4, 73-79 (2006).
- [28] A. Cheng, J. T. Gonçalves, P. Golshani, K. Arisaka, and C. Portera-Cailliau, "Simultaneous two-photon calcium imaging at different depths with spatiotemporal multiplexing," NAT METHODS 8, 139 (2011).
- [29] W. Akemann, J. C. C. O. Ger, C. Ventalon, B. Mathieu, S. E. P. D. E, and L. Bourdieu, "Fast spatial beam shaping by acousto-optic diffraction for 3D non-linear microscopy," OPT EXPRESS 23, 28191-28205 (2015).
- [30] X. L. Dean-Ben, S. Gottschalk, L. B. Mc, S. Shoham, and D. Razansky, "Advanced optoacoustic methods for multiscale imaging of in vivo dynamics," CHEM SOC REV 46, 2158-2198 (2017).
- [31] R. Prevedel, A. J. Verhoef, A. J. Pernia-Andrade, S. Weisenburger, B. S. Huang, T. Nobauer, A. Fernandez, J. E. Delcour, P. Golshani, A. Baltuska, and A. Vaziri, "Fast volumetric calcium imaging across multiple cortical layers using sculpted light," NAT METHODS 13, 1021-1028 (2016).
- [32] M. B. Bouchard, V. Voleti, C. S. Mendes, C. Lacefield, W. B. Grueber, R. S. Mann, R. M. Bruno, and E. M. Hillman, "Swept confocally-aligned planar excitation (SCAPE) microscopy for high speed volumetric imaging of behaving organisms," NAT PHOTONICS 9, 113-119 (2015).
- [33] R. M. Power, and J. Huisken, "A guide to light-sheet fluorescence microscopy for multiscale imaging," NAT METHODS 14, 360-373 (2017).
- [34] A. L. P. S. Carlos Cruz Perez, "Calcium neuroimaging in behaving zebrafish larvae using a turn-key light field camera," J BIOMED OPT 20, 20 (2015).
- [35] R. Prevedel, "Simultaneous whole-animal 3D imaging of neuronal activity using light-field microscopy," NAT METHODS 11, 727 (2014).
- [36] X. L. Deán-Ben, T. F. Fehm, S. J. Ford, S. Gottschalk, and D. Razansky, "Spiral volumetric optoacoustic tomography visualizes multi-scale dynamics in mice," Light: Science & Amp; Applications 6, e16247 (2017).
- [37] Z. Chen, X. L. Deán-Ben, S. Gottschalk, and D. Razansky, "Hybrid system for in vivo epifluorescence and 4D optoacoustic imaging," OPT LETT 42, 4577-4580 (2017).
- [38] A. O. Zbek, X. E. L. I. De A N-Ben, and D. Razansky, "Optoacoustic imaging at kilohertz volumetric frame rates," OPTICA 5, 857-863 (2018).
- [39] Z. Chen, X. E. L. I. De A N-Ben, S. Gottschalk, and D. Razansky, "Performance of optoacoustic and fluorescence imaging in detecting deep-seated fluorescent agents," BIOMED OPT EXPRESS 9, 2229-2239 (2018).
- [40] E. Wang, C. M. Babbey, and K. W. Dunn, "Performance comparison between the high-speed Yokogawa spinning disc confocal system and single-point scanning confocal systems," J Microsc 218, 148-159 (2005).
- [41] R. Graf, J. Rietdorf, and T. Zimmermann, "Live cell spinning disk microscopy," Adv Biochem Eng Biotechnol 95, 57-75 (2005).
- [42] F. Bergermann, L. Alber, S. J. Sahl, J. Engelhardt, and S. W. Hell, "2000-fold parallelized dual-color STED fluorescence nanoscopy," OPT EXPRESS 23, 211-223 (2015).
- [43] J. N. Stirman, I. T. Smith, M. W. Kudenov, and S. L. Smith, "Wide field-of-view, multi-region, two-photon imaging of neuronal activity in the mammalian brain," NAT BIOTECHNOL 34, 857 (2016).
- [44] L. Song, H. Lu-Walther, R. Förster, A. Jost, M. Kielhorn, J. Zhou, and R. Heintzmann, "Fast structured illumination microscopy using rolling shutter cameras," MEAS SCI TECHNOL 27, 55401 (2016).
- [45] P. W. Winter, A. G. York, D. D. Nogare, M. Ingaramo, R. Christensen, A. Chitnis, G. H. Patterson, and H. Shroff, "Two-photon instant structured illumination microscopy improves the depth penetration of super-resolution imaging in thick scattering samples," OPTICA 1, 181-191 (2014).
- [46] A. G. York, P. Chandris, D. D. Nogare, J. Head, P. Wawrzusin, R. S. Fischer, A. Chitnis, and H. Shroff, "Instant super-resolution imaging in live cells and embryos via analog image processing," NAT METHODS 10, 1122 (2013).
- [47] M. Ingaramo, A. G. York, P. Wawrzusin, O. Milberg, A. Hong, R. Weigert, H. Shroff, and G. H. Patterson, "Two-photon excitation improves multifocal structured illumination microscopy in thick scattering tissue," Proc Natl Acad Sci U S A 111, 5254-5259 (2014).
- [48] V. Kalchenko, D. Israeli, Y. Kuznetsov, and A. Harmelin, "Transcranial optical vascular imaging (TOVI) of cortical hemodynamics in mouse brain," Sci Rep 4, 5839 (2014).
- [49] G. R. B. E. Römer, and P. Bechtold, "Electro-optic and Acousto-optic Laser Beam Scanners," Physics Procedia 56, 29-39 (2014).